Transgenerational Epigenetic Inheritance Factors Localize to Spatially and Temporally Ordered Liquid Droplet Assemblages

Gang Wan[1]*, Brandon D. Fields[1,2]*, George Spracklin[1,2], Carolyn Phillips[3], Scott Kennedy[1]

[1] Department of Genetics, Harvard Medical School, Boston, MA 02115, USA

[2] Laboratory of Genetics, University of Wisconsin-Madison, Madison, WI 53706, USA

[3] Department of Biological Sciences, University of Southern California, Los Angeles, CA 90089, USA

*These authors contributed equally to this work.

Abstract:

Epigenetic information can be inherited for multiple generations (termed transgenerational epigenetic inheritance or TEI)[1,2]. Non-coding RNAs have emerged as important mediators of TEI, although the mechanism(s) by which non-coding RNAs mediate TEI remains poorly understood. dsRNA-mediated gene silencing (RNAi) in *C. elegans* is a robust example of RNA-directed TEI[3–5]. To further our understanding of RNA-directed TEI, we conducted a genetic screen in *C. elegans* to identify genes required for RNAi inheritance. Our screen identified the conserved RNA helicase/Zn finger protein ZNFX-1 and the Argonaute protein WAGO-4. We find that WAGO-4 and ZNFX-1 act cooperatively in inheriting generations to mark mRNAs of genes undergoing heritable silencing to maintain small interfering (si)RNA expression across generations. Additionally, we find that ZNFX-1/WAGO-4 localize to a liquid droplet organelle termed the P granule in early germline blastomeres. Later in development, ZNFX-1/WAGO-4 demix from P granule components to form an independent liquid droplet organelle that we term the Z granule. In the adult germline, Z granules assemble into ordered tri-droplet assemblages with P granules and another germline droplet-like foci termed the *Mutator* foci. This work identifies conserved RNA-binding proteins that contribute to RNA-directed TEI in *C. elegans*, defines a liquid droplet organelle termed the Z granule, and shows that liquid droplet organelles can undergo developmentally regulated cycles of mixing/demixing and assemble into spatially ordered multi-droplet structures. We speculate that temporal and spatial ordering of liquid droplets helps cells organize and coordinate the complex RNA processing pathways underlying gene regulatory systems, such as RNA-directed TEI.

Previous genetic screens have identified several components of the *C. elegans* RNAi inheritance machinery [5–7]. We conducted a modified genetic screen designed to identify additional RNAi inheritance factors (Fig. S1). Our screen identified 37 mutations that disrupted RNAi inheritance. We subjected DNA from these 37 mutant strains to whole-genome sequencing and identified four independent mutations in the gene *zk1067.2* (Fig. 1A). To confirm that *zk1067.2* is required for RNAi inheritance, we tested two additional alleles of *zk1067.2* (*gk458570* and *gg561*) for RNAi inheritance defects. Treatment of *C. elegans* with *gfp* dsRNA (*gfp* RNAi) can trigger silencing of germline expressed *gfp* reporter genes for multiple generations [3,5,7]. *gk458570* and *gg561* animals responded like wild-type animals to treatment with *gfp* dsRNA, however, progeny of these mutant animals were unable to inherit gene silencing (Fig. 1B, and Fig. S2). Additionally, animals harboring *zk1067.2* mutations were defective for RNAi inheritance when the *dpy-11* and *oma-1* genes were targeted with dsRNA (Fig. S3). We conclude that *zk1067.2* is required for RNAi inheritance.

Sequence analysis showed that ZK1067.2 encodes a 2443 amino acid protein that contains a superfamily one (SF1) RNA helicase domain and a Zn finger domain (Fig. 1A). A single putative orthologue of ZK1067.2 was found in most eukaryotic genomes. The *S. pombe* homolog of ZK1067.2 (termed HRR1) is a nuclear protein that physically interacts with Argonaute (AGO) and RNA Dependent RNA Polymerase (RdRP) to direct pericentromeric heterochromatin [8]. The *N. crassa* homolog (SAD-3) is a cytoplasmic protein required for an RNAi-related phenomenon termed meiotic silencing of unpaired DNA (MSUD) [9]. Homology between ZK1067.2 and its mammalian ortholog ZNFX1 extend to a Zn finger domain not present in fungal orthologues. We conclude that ZK1067.2 is a conserved protein that is involved in small RNA-mediated gene silencing in many eukaryotes. Henceforth, we refer to ZK1067.2 as ZNFX-1.

To begin to understand the function of ZNFX-1 during RNAi inheritance, we used CRISPR/Cas9 to insert a *3xflag::gfp* epitope immediately upstream of the *znfx-1* start codon. *3xflag::gfp::znfx-1* animals behaved like wild-type animals during RNAi inheritance assays, indicating that *3xflag::gfp::znfx-1* encodes a functional protein (Fig. S4). [Note, CRISPR-mediated gene conversion was used to epitope tag the genes described in this work and the resultant fusion proteins were functional for RNAi inheritance unless otherwise stated (also see Fig. S4)]. We observed GFP::ZNFX-1 expression in the adult germline as well as in

developing germ cells during all stages of embryonic and larval development (Fig. 1C, and data not shown). No GFP::ZNFX-1 expression was observed in somatic tissues. Post fertilization, *C. elegans* zygotes undergo a series of asymmetric cell divisions in which germline determinants segregate with the germline blastomeres of the P lineage. During embryonic development, ZNFX-1 foci were concentrated in, and segregated with, the germline P blastomeres (Fig 1C). In adult germ cells, GFP::ZNFX-1 was concentrated in foci that were distributed in a perinuclear pattern around germ cell nuclei (Fig 1D). We conclude that *znfx-1* encodes a germline-expressed protein that segregates with the germline and localizes to perinuclear foci in adult germ cells.

ZNFX-1 could act in the parental generation to initiate RNAi inheritance or in progeny to receive RNAi inheritance signals (or both). The following results demonstrate that ZNFX-1 acts in inheriting generations to promote the memory of RNAi. We initiated gene silencing in *znfx-1/+* heterozygous animals and scored the +/+ and -/- progeny for their ability to inherit gene silencing. Progeny harboring at least one wild-type copy of *znfx-1* were capable of inheriting gene silencing while -/- progeny were not (Fig. 1E). When we initiated gene silencing in *znfx-1(-/-)* animals, introduced a wild-type copy of *znfx-1* to progeny (via mating), and scored *znfx-1/+* cross-progeny for inheritance, we found that *znfx-1(+/-)* progeny were able to inherit silencing (Fig. S5). These data suggest that *znfx-1* acts in inheriting generations to enable RNAi inheritance. The following molecular data support this idea. First, treatment of animals with *oma-1* dsRNA silences the *oma-1* mRNA for multiple generations [4,5]. We used qRT-PCR to measure *oma-1* mRNA and pre-mRNA levels in *znfx-1(-)* animals exposed to *oma-1* RNAi, as well as in the progeny of these animals. *znfx-1(-)* animals responded normally to *oma-1* RNAi; however, their progeny failed to inherit silencing (Fig. 1F). Second, the nuclear RNAi factor NRDE-2 binds to pre-mRNA of genes undergoing heritable silencing [5]. When *znfx-1(-)* animals were exposed directly to *oma-1* dsRNA, NRDE-2 bound to the *oma-1* pre-mRNA at wild-type levels, however, in progeny of *znfx-1(-)* mutant animals NRDE-2 failed to bind *oma-1* pre-mRNA (Fig. S6). Third, during RNAi inheritance, siRNAs with sequence complementarity to genes undergoing RNAi silencing are expressed for multiple generations [5]. In *znfx-1(-)* animals exposed directly to *oma-1* dsRNA, *oma-1* siRNAs were produced at wild-type levels; however, the progeny of *znfx-1(-)* animals failed to express *oma-1* siRNAs (Fig. 1G). Together these data establish that ZNFX-1 is a dedicated RNAi inheritance factor.

The *C. elegans* genome encodes ~27 Argonaute (AGO) proteins. The molecular function of most of these AGOs remains a mystery. Two of the mutant strains identified by our genetic screen harbored mutations in the AGO-encoding gene *wago-4*. To confirm WAGO-4 is required for RNAi inheritance, we tested two additional *wago-4* deletion alleles (*tm1019* and *tm2401*) for RNAi inheritance defects. Both alleles exhibited RNAi inheritance defects (Fig. 1B and S7). Thus, like ZNFX-1, WAGO-4 is required for RNAi inheritance. Additionally, when we appended a *gfp* tag to the *wago-4* locus, we observed that, like ZNFX-1, WAGO-4 is a germline-expressed protein that segregates with the P lineage blastomeres and localizes to perinuclear foci (Fig. S7). For unknown reasons, our GFP::WAGO-4 fusion protein was fully functional for RNAi inheritance in some RNAi inheritance assays but only partially functional in other assays (Fig. S8). TagRFP::ZNFX-1 and GFP::WAGO-4 colocalized in germ cells, hinting that WAGO-4 and ZNFX-1 may act together to promote RNAi inheritance (Fig. 2A). Four additional lines of evidence support this idea. First, *znfx-1*; *wago-4* double mutant animals behaved like single mutant animals in an RNAi inheritance assay, indicating *wago-4* and *znfx-1* are part of the same genetic pathway (Fig. 2B). Second, WAGO-4 and ZNFX-1 co-precipitate, suggesting a physical interaction between the two proteins (Fig. 2C). Third, *wago-4* mutant animals behaved like *znfx-1* mutant animals in molecular assays of RNAi inheritance. For instance, following *oma-1* RNAi, *wago-4* mutant animals express wild-type levels of *oma-1* siRNAs; however, progeny of *wago-4* mutant animals fail to inherit these small RNAs (Fig. 1G). Finally, ZNFX-1 and WAGO-4 share a pleiotropy: Both *znfx-1* and *wago-4* mutant animals exhibit a temperature-sensitive mortal germline (Mrt) phenotype, whereby mutant animals became sterile several generations after populations were shifted to a higher temperature (25C) (Fig. 2D). Taken together these data show that WAGO-4 functions with ZNFX-1 to transmit RNA-based epigenetic information across generations.

How do WAGO-4 and ZNFX-1 promote RNAi inheritance? The closest homolog of ZNFX-1 is the RNA helicase SMG-2/UPF1, which binds and marks mRNAs containing premature termination codons [10]. We wondered if, by analogy, ZNFX-1 might bind and mark mRNAs encoded by genes undergoing heritable gene silencing. To test this idea, we subjected 3XFLAG::ZNFX-1 expressing animals to *oma-1* RNAi, immunoprecipitated 3XFLAG::ZNFX-1, and used qRT-PCR to ask if *oma-1* RNAi directed ZNFX-1 to bind the *oma-1* mRNA. Indeed, *oma-1* RNAi caused ZNFX-1 to co-precipitate with *oma-1* mRNA (Fig. 2E). The following data argue that the binding of ZNFX-1 to mRNA is a sequence-specific event directed by the RNAi

machinery. First, RNAi targeting the *lin-15b* gene caused ZNFX-1 to bind the *lin-15b* mRNA, but not the *oma-1* mRNA (and vice versa), indicating that ZNFX-1/mRNA interactions are sequence-specific (Fig. S9). Second, most RNA helicases bind RNA via their helicase domains. Deletion of the ZNFX-1 helicase domain did not affect ZNFX-1 expression (not shown) but did prevent ZNFX-1 from binding *oma-1* mRNA (Fig. 2E). Third, AGO proteins (like WAGO-4) use small RNA cofactors to direct sequence-specific RNA interactions. In *wago-4* mutant animals, ZNFX-1 failed to bind the *oma-1* mRNA in response to *oma-1* RNAi (Fig. 2E). We conclude that RNAi directs ZNFX-1 to bind mRNAs undergoing heritable silencing and that the AGO protein WAGO-4 is required for this property of ZNFX-1.

P granules are liquid droplet organelles that, like ZNFX-1/WAGO-4 foci, segregate with the germline blastomeres (P_0-P_4) during embryonic development [11,12]. The low-complexity domain containing protein PGL-1 marks P granules [13]. Both GFP::ZNFX-1 and GFP::WAGO-4 colocalized with PGL-1::TagRFP in P_1-P_3 germline blastomeres, suggesting that ZNFX-1 and WAGO-4 are P granule factors (Fig. 3A). MEG-3 and MEG-4 are low-complexity domain proteins that are redundantly required for P granule formation in the embryonic P lineage of *C. elegans* (Fig. 3B) [14]. In *meg-3/4*(-) embryos, ZNFX-1/WAGO-4 foci failed to form in the germline blastomeres (Fig. 3B). Thus, in early P_1-P_3 germline blastomeres, ZNFX-1 and WAGO-4 localize to P granules.

At the ~100 cell stage of embryonic development the P_4 blastomere divides to give rise to Z2 and Z3, which are the primordial germ cells of *C. elegans*. Surprisingly, we found that GFP::ZNFX-1 no longer colocalized with PGL-1::TagRFP in Z2/Z3 (Fig. 3C). Rather, GFP::ZNFX-1 appeared in foci that were adjacent to (see below), yet distinct from, PGL-1::TagRFP foci (Fig. 3C). Quantitative analyses showed that the degree to which ZNFX-1 and PGL-1 colocalized changed during development, with a transition from colocalized to non-colocalized states occurring between the P_3 and Z2/Z3 stage of germline development (Fig. 3D). Conversely, GFP::WAGO-4 and TagRFP::ZNFX-1 remain colocalized throughout germline development (Fig. 3C and 3D). Thus, ZNFX-1/WAGO-4 and PGL-1 transition from colocalized to non-colocalized at some point between P_3 and Z2/Z3. This transition could result from the formation of new foci or from demixing of factors within existing P granules. We favor the later model as time-lapse imaging in early Z2/Z3 cells captured ZNFX-1 and PGL-1 demixing events

(Fig. 3E). We conclude that ZNFX-1 and WAGO-4 demix from P granule constituents early in embryonic development.

Liquid droplets organelles (such as the *C. elegans* P granules) are self-assembling cellular structures that form when specific proteins and RNAs undergo liquid-liquid phase transitions from surrounding cytoplasm. The ability of ZNFX-1 and WAGO-4 to demix from P granules hints that foci labeled by ZNFX-1/WAGO-4 (post Z2/Z3) may also be liquid droplets. Liquid droplets are typically spherical in shape and capable of flowing as distinct entities through other liquids, such as the cytoplasm. Consistent with the idea that ZNFX-1 foci are liquid droplets, in maturing oocytes ZNFX-1 foci assumed spherical shapes, detached from nuclei, and flowed through the cytoplasm (Fig. 4A). Additionally, constituents of liquid droplets undergo rapid internal rearrangements [15,16]. Fluorescence recovery after photobleaching (FRAP) experiments showed that in ZNFX-1 foci, GFP::ZNFX-1 fluorescence recovered from bleaching rapidly (t=~8 seconds), which is a rate similar to that reported for PGL-1 FRAP in P granules (Fig. 4B) [11]. Taken together, these data show that the foci labeled by ZNFX-1 and WAGO-4 (post Z2/Z3) are liquid droplets, which we now refer to as Z granules.

C. elegans germ cells possess at least two other foci (in addition to P granules) with properties akin to liquid droplets (processing bodies and *Mutator* foci)[17,18]. TagRFP::ZNFX-1 did not co-localize with MUT-16::GFP, which marks *Mutator* foci, nor did GFP::ZNFX-1 colocalize with mCherry::PATR-1 or mRuby::DCAP-1, which marks processing bodies (Fig. 5A and Fig. S10). Interestingly, although Z granules did not colocalize with *Mutator* foci the locations of these two foci were not random. Z granules were usually [89% of the time, (n=35)] found closely apposed to (no empty space observable between fluorescence signals) a *Mutator* foci (Fig. 5A). Similarly, Z granules were usually [91% of the time, (n=35)] found closely apposed to a P granule (Fig. 5A). EGO-1 is another marker of P granules [17,19]. Z granules localized adjacent to, yet were distinct from, EGO-1 foci (Fig. S11). Quantification of distances between surfaces and centers of fluorescence for the three foci supported the idea that Z granules localize adjacent to P granules and *Mutator* foci in adult germ cells (Fig. 5B). This analysis also showed that the distance between the surfaces of Z granules and P granules/*Mutator* foci (but not P granules and *Mutator* foci) lies within the diffraction limit of light (zero distance values), indicating that Z granules exist in very close proximity to, and may be in direct physical contact with P granules and *Mutator* foci (Fig. 5B). Note, although Z granules are intimately associated with P

granules/*Mutator* foci in adult germ cells (and throughout most of germline development), they can exist independently. For instance, in the adult germline, P granules disappear during oocyte maturation (Fig.4A). Z granules remained visible at developmental time points when P granules were no longer present (Fig. 4A). Similarly, Z granules are present in developing germ cells at time points (*i.e.* P blastomeres) when *Mutator* foci are not thought to be present [17]. Shearing forces cause P granules in pachytene stage germ cells to disengage from nuclei and flow through the germline syncytium [11]. After applying shearing force, we found that P granules flowed through the cytoplasm, however, Z granules remained static (Fig. S12). Thus, Z granules can be separated from P granules and *Mutator* foci developmentally and physically. We conclude that Z granules represent an independent form of liquid droplets, which closely mirror P granules and *Mutator* foci in adult germ cells.

Our data suggest that Z granules may localize between (bridge) P granules and *Mutator* foci. To test this idea, we imaged the three foci simultaneously using PGL-1::mCardinal, TagRFP::ZNFX-1, and MUT-16::GFP expressing animals[20]. This analysis confirmed the idea that Z granules bridge P granules and *Mutator* foci (Fig. 5C): In 60% (52/86) of cases, we observed a Z granule in close apposition to both a P granule and a Mutator, while in 92% (48/52) of these cases the Z granule lay between the other two foci. In no case (0/52) did a P granule or a *Mutator* foci bridge the other two types of foci, respectively. Quantification of the distances between the centers and surfaces of Z granules, P granules, and *Mutator* foci from triple-marked images support the idea that Z granules act as a bridge between P granules and Mutator foci in adult germ cells (Fig. S13). We conclude that P granules, Z granules, and *Mutator* foci form tri-droplet assemblages (henceforth PZMs) in adult germ cells and that the relative position of the three liquid droplets constituting the PZM is ordered.

Here we show that the inheritance factors ZNFX-1 and WAGO-4 localize to a liquid droplet organelle that we name the Z granule. Thus, one function of the Z granule is to concentrate and segregate silencing factors into the germline to promote RNA-based TEI. ZNFX-1 is a conserved Zn finger RNA helicase, which, in *C. elegans*, marks RNAs produced by genes undergoing heritable silencing. The *S. pombe* ortholog of ZNFX-1 is Hrr1, which forms a nuclear complex (termed the RDRC) with Argonaute, the nucleotidyltransferase Cid12, and RdRP to amplify small RNA populations directing pericentromeric heterochromatin [8]. We speculate that in *C. elegans* the RDRC has migrated from the nucleus to the Z granule promotes where it

promotes RNAi inheritance in *C. elegans* by: 1) binding inherited siRNAs (via WAGO-4), 2) marking mRNAs complementary to inherited siRNAs (via WAGO-4 and ZNFX-1), 3) using marked mRNAs as templates to amplify siRNA populations (via recruitment of one of the four *C. elegans* RdRP enzymes), and 4) repeating this cycle each generation (Fig. S14). Support for this model comes from the recent identification of a homologue of the *S. pombe* RDRC factor CID12 (PUP-1/CDE-1) as a *C. elegans* RNAi inheritance factor [6]. ZNFX-1 and WAGO-4 demix from components of the P granule during early embryogenesis to form independent liquid droplets. Demixing occurs at a developmental time that correlates roughly with the first association of P granules with nuclear pores and the advent of germline transcription [12,21,22]. We speculate that demixing might be triggered when newly synthesized mRNAs transit P granules and interact with RNA binding proteins to alter local protein concentration and precipitate demixing. In addition to temporal ordering, we find that Z granules are spatially ordered relative to P granules and *Mutator* foci, with Z granules forming the centerpiece of PZM tri-droplet assemblages in adult germ cells. These results show that cells possess mechanism(s) to organize and arrange liquid droplets in space as well as time. Additional work is needed to understand how PZM segments assemble in the correct order and if/how ordered PZM assembly contributes to RNA-based TEI. We note, however, that small RNA-related factors from each of the three PZM segments have now been linked to TEI in *C. elegans*, suggesting that ordered PZM assembly is likely an important facet of RNA-directed TEI [6,7,23] (Fig. S15). Small RNA-mediated gene regulatory pathways in animals are highly complex with thousands of small RNAs (*e.g.* miRNAs, piRNAs, siRNAs) regulating thousands of mRNAs at virtually all levels of gene expression. We speculate that the ordering of liquid droplet organelles in space and time helps organize and coordinate the complex RNA processing steps that underlie RNA-directed TEI (Fig. S14). Similar strategies may be used by cells to organize and coordinate other gene regulatory pathways.

Bibliography:

1. Heard, E. & Martienssen, R. A. Transgenerational epigenetic inheritance: myths and mechanisms. *Cell* **157,** 95–109 (2014).

2. Lim, J. P. & Brunet, A. Bridging the transgenerational gap with epigenetic memory. *Trends Genet.* **29,** 176–186 (2013).

3. Vastenhouw, N. L. *et al.* Gene expression: long-term gene silencing by RNAi. *Nature* **442,** 882 (2006).

4. Alcazar, R. M., Lin, R. & Fire, A. Z. Transmission dynamics of heritable silencing induced by double-stranded RNA in Caenorhabditis elegans. *Genetics* **180,** 1275–1288 (2008).

5. Buckley, B. A. *et al.* A nuclear Argonaute promotes multigenerational epigenetic inheritance and germline immortality. *Nature* **489,** 447–451 (2012).

6. Spracklin, G. *et al.* The RNAi Inheritance Machinery of Caenorhabditis elegans. *Genetics* **206,** 1403–1416 (2017).

7. Ashe, A. *et al.* piRNAs can trigger a multigenerational epigenetic memory in the germline of C. elegans. *Cell* **150,** 88–99 (2012).

8. Motamedi, M. R. *et al.* Two RNAi complexes, RITS and RDRC, physically interact and localize to noncoding centromeric RNAs. *Cell* **119,** 789–802 (2004).

9. Hammond, T. M. *et al.* SAD-3, a Putative Helicase Required for Meiotic Silencing by Unpaired DNA, Interacts with Other Components of the Silencing Machinery. *G3* **1,** 369–376 (2011).

10. Brogna, S., McLeod, T. & Petric, M. The Meaning of NMD: Translate or Perish. *Trends Genet.* **32,** 395–407 (2016).

11. Brangwynne, C. P. *et al.* Germline P granules are liquid droplets that localize by controlled dissolution/condensation. *Science* **324,** 1729–1732 (2009).

12. Strome, S. & Wood, W. B. Generation of asymmetry and segregation of germ-line granules in early C. elegans embryos. *Cell* **35,** 15–25 (1983).

13. Strome, S. & Wood, W. B. Immunofluorescence visualization of germ-line-specific cytoplasmic granules in embryos, larvae, and adults of Caenorhabditis elegans. *Proc. Natl. Acad. Sci. U. S. A.* **79,** 1558–1562 (1982).

14. Wang, J. T. *et al.* Regulation of RNA granule dynamics by phosphorylation of serine-rich, intrinsically disordered proteins in C. elegans. *Elife* **3,** e04591 (2014).

15. Toretsky, J. A. & Wright, P. E. Assemblages: functional units formed by cellular phase separation. *J. Cell Biol.* **206,** 579–588 (2014).

16. Weber, S. C. & Brangwynne, C. P. Getting RNA and protein in phase. *Cell* **149,** 1188–1191 (2012).

17. Phillips, C. M., Montgomery, T. A., Breen, P. C. & Ruvkun, G. MUT-16 promotes formation of perinuclear mutator foci required for RNA silencing in the C. elegans germline. *Genes Dev.* **26,** 1433–1444 (2012).

18. Gallo, C. M., Munro, E., Rasoloson, D., Merritt, C. & Seydoux, G. Processing bodies and germ granules are distinct RNA granules that interact in C. elegans embryos. *Dev. Biol.* **323,** 76–87 (2008).

19. Claycomb, J. M. *et al.* The Argonaute CSR-1 and its 22G-RNA cofactors are required for holocentric chromosome segregation. *Cell* **139,** 123–134 (2009).

20. Chu, J., Haynes, R. D., Corbel, S. Y. & Li, P. Non-invasive intravital imaging of cellular differentiation with a bright red-excitable fluorescent protein. *Nature* (2014).

21. Seydoux, G. & Dunn, M. A. Transcriptionally repressed germ cells lack a subpopulation

of phosphorylated RNA polymerase II in early embryos of Caenorhabditis elegans and Drosophila melanogaster. *Development* **124,** 2191–2201 (1997).

22. Furuhashi, H. *et al.* Trans-generational epigenetic regulation of C. elegans primordial germ cells. *Epigenetics Chromatin* **3,** 15 (2010).

23. Shirayama, M. *et al.* piRNAs initiate an epigenetic memory of nonself RNA in the C. elegans germline. *Cell* **150,** 65–77 (2012).

24. McNally, K., Audhya, A., Oegema, K. & McNally, F. J. Katanin controls mitotic and meiotic spindle length. *J. Cell Biol.* **175,** 881–891 (2006).

25. Farboud, B. & Meyer, B. J. Dramatic enhancement of genome editing by CRISPR/Cas9 through improved guide RNA design. *Genetics* **199,** 959–971 (2015).

26. Arribere, J. A. *et al.* Efficient marker-free recovery of custom genetic modifications with CRISPR/Cas9 in Caenorhabditis elegans. *Genetics* **198,** 837–846 (2014).

27. Gent, J. I. *et al.* A Caenorhabditis elegans RNA-directed RNA polymerase in sperm development and endogenous RNA interference. *Genetics* **183,** 1297–1314 (2009).

28. Ollion, J., Cochennec, J., Loll, F., Escudé, C. & Boudier, T. TANGO: a generic tool for high-throughput 3D image analysis for studying nuclear organization. *Bioinformatics* **29,** 1840–1841 (2013).

29. Bolte, S. & Cordelières, F. P. A guided tour into subcellular colocalization analysis in light microscopy. *J. Microsc.* **224,** 213–232 (2006).

Materials and Methods:

Strain list: N2 (CGC); (YY009) *eri-1*(*mg366*), (YY193) *eri-1*(*mg366*); *nrde-2*(*gg91*), (YY502) *nrde-2*(*gg91*), (YY503) *nrde-2*(*gg90*), (YY538) *hrde-1*(*tm1200*), (YY562) *hrde-1*(*tm1200*); *oma-1*(*zu405*), (YY913) *nrde-2*(*gg518*[*nrde-2::3xflag::ha*]), (YY916) *znfx-1*(*gg544*[*3xflag::gfp::znfx-1*]), (YY947) *hrde-1*(*tm1200*); *nrde-2*(*gg518*), (YY967) *pgl-1*(*gg547*[*pgl-1::3xflag::tagrfp*]), (YY968) *znfx-1*(*gg544*); *pgl-1*(*gg547*), (YY996) *znfx-1*(*gg561*), (TX20) *oma-1*(*zu405*), (YY998) *znfx-1*(*gg544*)*; ego-1*(*gg644*[*ha::tagrfp::ego-1*]), (YY1020) *znfx-1*(*gg561*); *oma-1*(*zu405*), (SX461) *mjIS31*(*pie-1::gfp::h2b*), (SS579) *pgl-1*(*bn101*), (JH3225) *meg-3*(*tm4259*); *meg-4*(*ax2026*), (DG3226) *deps-1*(*bn124*), (YY1006) *eri-1*(*mg366*); *znfx-1*(*gg561*), (YY1003) *eri-1*(*mg366*); *znfx-1*(*gk458570*), (YY1021) *znfx-1*(*gg561*); *nrde-2*(*gg518*), (YY1062) *znfx-1* (*gk458570*), (YY1081) *deps-1*(*bn124*); *mjIS31,* (YY1083) *wago-4*(*tm1019*), (YY1084) *wago-4*(*tm2401*), (YY1093) *wago-4*(*tm1019*); *mjIS31,* (YY1094) *wago-4*(*tm2401*); *mjIS31,* (YY1108) *znfx-1*(*gg561*); *mjIS31*, (YY1109) *mjIS31*; *dpy-10*(*cn64*), (YY1110) *eri-1*(*mg366*); *wago-4*(*tm1019*), (YY1111) *eri-1*(*mg366*); *wago-4*(*tm2401*), (YY1153) *wago-4*(*tm1019*), *znfx-1*(*gg544*), (YY1155) *rde-1*(*ne219*); *znfx-1*(*gg544*), (YY1265) *rde-1*(*ne219*); *mjIS31*, (YY1287) *znfx-1*(*gg611*[*ha::znfx-1*]), (YY1305) *meg-3*(*tm4259*); *meg-4*(*ax2026*), *znfx-1*(*gg544*), (YY1308) *meg-3*(*tm4259*); *meg-4*(*ax2026*), *pgl-1*(*gg547*), (YY1325) *wago-4*(*gg620*[*3xflag::gfp::wago-4*]), (YY1327) *pgl-1*(*gg547*); *wago-4*(*gg620*), (YY1364) *meg-3*(*tm4259*); *meg-4*(*ax2026*), *wago-4*(*gg620*), (YY1388) *wago-4*(*gg627*[*3xflag::wago-4*]), (YY1393) *znfx-1*(*gg611);* *wago-4*(*gg627),* (YY1403) *wago-4*(*tm1019*); *znfx-1*(*gg561*), (YY1408) *znfx-1*(*gg561*); *mjIS31*; *dpy-10*(*cn64*), (YY1416) *znfx1*(*gg544*); axIs1488, (YY1419) *znfx-1*(*gg561*); *wago-4*(*tm1019*); *oma-1*(*zu405*), (YY1442) *znfx1*(*gg544*); hjSi397, (YY1446) *znfx-1*(*gg634*[*ha::tagrfp::znfx-1*]), (cmp3) *mut-16::gfp::flag+loxP,* (YY1444) *znfx-1*(*gg634*); *mut-16*[*mut-16::gfp::flag+loxP*], (YY1452) *znfx-1*(*gg544*); *ltIs37*(*pie-1::mcherry::his58*), (YY1453) *znfx-1*(*gg634*); *wago-4*(*gg620*), (YY1486) *znfx1*(*gg631*[*3xflag::gfp::znfx-1* Δ *helicase*]), (YY1491) *wago-4*(*gg620*)*; oma-1*(*zu405*) （YY1492）*pgl-1*(*gg640*[*pgl-1::3xflag::mcardinal*]); *mut-16*[*mut-16::gfp::flag+loxP*]; *znfx-1*(*gg634*), (YY1503) *pgl-1*(*gg547*); *mut-16*[*mut-16::gfp::flag+loxP*].

CRISPR/Cas9: gRNAs were chosen using Ape according to following standards: first, PAM sites are in the context of GGNGG [25] or GNGG; second, GC content of 20 bp spacer sequence was 40% to 60%; third, high specificity according to crispr.mit.edu. All CRISPR was done using co-CRISPR strategy [26]. Plasmids were purified with PureLink™ HiPure Plasmid Kits (Thermofisher). For deletions: two gRNAs (20ng/μl) were co-injected into gonads with pDD162(50ng/μl), *unc-58* gRNA(20ng/μl), AF-JA-76 (20ng/μl) and 1X taq buffer. For 3xFLAG or HA epitope tagging, single strand oligos (4nM ultramer from IDT, purified by isopropanol precipitation) with 50bp homology regions were used as repair templates. gRNA (20ng/μl) and repair template (20ng/μl) were co-injected into gonads with pDD162(50ng/μl), *unc-58* gRNA(20ng/μl), AF-JA-76 (20ng/μl) and 1X taq buffer. For GFP, tagRFP or mCardinal tagging, repair templates contained homologous arms of 500bp to 1000bp and were cloned into pGEM-7zf(+). Sequences were confirmed by Sanger sequencing. Repair templates were amplified with PCR, gel purified and isopropanol precipitated. PCR product was heated at 95 ℃

for 5min and then immediately put on ice for at least 2min. Injection mix was prepared: pDD162(50ng/µl), *unc-58* gRNA (20ng/µl), AF-JA-76(20ng/µl), gRNAs close to N terminal or C terminal of the genes (20ng/µl), heated and cooled repair template (50ng/µl) and 1X standard taq buffer. Injected animals were maintained at 25°C, Unc animals were isolated 4 days later and grown at 20℃. Animals were screened for deletion or tagging by PCR.

RNA IP: Animals were flash frozen in liquid nitrogen and stored at -80℃. Animals were resuspended in sonication buffer (20 mM Tris.HCl PH 7.5, 200mM NaCl, 2.5mM MgCl2, 10% glycerol, 0.5% NP-40, 80U/ml RNaseOUT, 1mM DTT and protease inhibitor cocktail without EDTA) and sonicated (30s on, 30s off, 20%-30% output for 2min on a Qsonica Q880R sonicator, repeat once). Lysates were clarified by centrifuging at 14000 rpm for 15min. Supernatants were precleared with protein A agarose beads and incubated with FLAG-M2 agarose beads for 2 hours at 4℃. Beads were washed with RIP buffer (20 mM Tris.HCl PH 7.5, 200mM NaCl, 2.5mM MgCl2, 10% glycerol, 0.5% NP-40) 6x. Protein and associated RNAs were eluted with 100ug/ml 3xFLAG peptide. RNAs were treated with Turbo DNase I for 20 min at 37°C and then extracted with TRIzol reagent followed by precipitation with isopropanol.

RT-qPCR: mRNA isolated from total RNA or from RNA IP experiments, was converted to cDNA using the iScript cDNA synthesis kit according to vendor's instructions. The following primer sequence were used to quantify mRNA levels. *oma-1* mRNA:GCTTGAAGATATTGCATTCAACC (Forward primer); AACTGTTGAAATGGAGGTGC (Reverse primer). *oma-1* pre-mRNA: GTGCGTTGGCTAATTTCCTG (Forward primer); CTGAATCGCGCGAACTTG (Reverse primer). *gld-2* mRNA: ACGTGTAGAAAGGGCTGCAC (Forward primer); GTCGATGCAGATGATGATGG (Reverse primer). *gld-2* pre-mRNA: CCTTATTAATTTCAGAGCTGCTGTC (Forward primer); AAGACTAGCACACGCAATCG (Reverse primer).

Mrt assay: Each generation, 3-6 L4 worms were picked to a single plate and grown at 25°C, average brood sizes were calculated by counting the total number of progeny per plate.

RNAi inheritance assays: *dpy-11* and *gfp* RNAi inheritance: Embryos were collected via hypochlorite treatment and placed onto HT115 bacteria expressing dsRNA against *dpy-11* or *gfp*. F1 embryos were collected by hypochlorite treatment from RNAi or control treated adults and placed onto non-RNAi plates. Worms were scored at late L4 (*dpy-11*) or early young adult (*gfp*) stages. *oma-1* RNAi inheritance: Experiments were done at 20°C. Embryos were collected via hypochlorite treatment and placed onto HT115 bacteria expressing dsRNA against *oma-1*. 6 F1 embryos were picked onto a single OP50 plate. From F2 to F6, 6 L4 animals were picked onto a single OP50 plate.

Co-immunoprecipitation: Young adults were flash frozen in liquid nitrogen. Animals were ground into powder in liquid nitrogen and resuspended in 1ml 1X lysis buffer (20mM Hepes pH7.5, 100mM NaCl, 5mM MgCl2, 1mM EDTA, 10% Glycerol, 0.25% Triton, 1mM fresh made PMSF, 1X complete protease inhibitor from Roche without EDTA) and rotated for 45min at 4℃.

Lysate was cleared by spinning at 5000 rpm for 15min, 30µl protein G beads were added to preclear lysate for 30min. 3xFLAG::WAGO-4 proteins were pulled down by 30µl agarose beads conjugated to α-FLAG antibody (A2220, Sigma-Aldrich). Input and IP proteins were separated by SDS-PAGE and detected by FLAG M2 antibody and HA antibody (Roche, 3F10).

Small RNA sequencing: Total RNA was extracted using TRIzol. 20ug total RNA were separated by 15% Urea gel. Small RNA from about 18 nt to 35 nt were cut from gel. Small RNAs were cloned using a 5' monophosphate independent small RNA protocol as previously described [27]. Libraries were multiplexed with a 4 nt 5' barcode and a 6 nt 3' barcode and pooled for next generation sequencing on a NextSeq 500. FastX 0.0.13 was used to separate reads that contained the 3' adapter and filter low quality reads for further analysis. Reads >14 nt were mapped to the *C. elegans* genome (WS220) using Bowtie. Read counts were normalized to the total number of reads matching the genome. Two independent libraries were prepared and the two replicates were combined for Figure 1.

Microscopy and Analysis: To image larval and adult stages, animals were immobilized in M9 with 0.1% Sodium Azide, and mounted on glass slides. To image embryos, gravid adults were dissected on a coverslip containing 10 µl of 1X egg buffer, and then mounted on freshly made 3% agarose pads. Animals were imaged immediately with a Nikon Eclipse Ti microscope equipped with a W1 Yokogawa Spinning disk with 50 um pinhole disk and an Andor Zyla 4.2 Plus sCMOS monochrome camera. A 60X/1.4 Plan Apo Oil objective was used unless otherwise stated.

Colocalization: The degree of colocalization between different fluorescently labeled proteins across development was calculated using the Coloc2 plugin from ImageJ. Animals were imaged as described above with the exception of using a 100X/1.45 Plan Apo Oil objective. 3-5 granules were selected from at least 3 different animals across each stage of development specified. Region of interest (ROI) masks were generated using the 3D ROI Manager plugin in ImageJ to eliminate black regions surrounding granules [28]. Coloc2 was used to generate a Pearson's R Value for degree of colocalization between two channels in region defined by the ROI mask.

FRAP: Fluorescence recovery after photobleaching (FRAP) experiments were conducted using a Zeiss LSM 780 point scanning confocal equipped with a Quasar PMT x2 + GAaSP 32 Channel Spectral Detector using a 63X/1.4 Plan Apo Oil objective. Adult animals (for pachytene germ cells) or embryos (for P2 blastomere) were suspended in a mixture of 0.5% sodium azide and 50% 0.1 µm polystyrene beads (Polysciences) to inhibit movement. The mixture was added to a coverslip and placed on a fresh 3% agarose pad. Slides were sealed with nail polish. The bleaching plugin within the Zeiss Black software was used to specify the ROI to be bleached. One ROI was used for all data points. Single z slice images were acquired at 1 second intervals for 15 seconds, followed by bleaching, then continued at 1 second intervals for 85 seconds. Images were aligned using neighboring granules in ImageJ to account for subtle shifts in movement. An ROI was generated around the bleached region and continuously measured

across all time points using the plot profile function within ImageJ. Data was normalized to an unbleached control granule to account for background bleaching throughout the 100 second period. Normalized data points were averaged across all 7 granules and plotted using Prism. The heat map of a representative granule was generated using the thermal LUT within ImageJ.

Quantification of distances between foci centers and surfaces. We imaged pachytene germ cell nuclei in 3 animals. ~10 granules were selected from each animal. Confocal z stacks were opened with the 3D objects counter plugin from ImageJ to generate x, y, and z coordinates for the center of each object [29]. To account for chromatic shift between channels, 0.1 µm Tetraspek beads were imaged and granule distances were corrected accordingly. Distances between foci surfaces was calculated with 3D ROI manager in ImageJ[28]. Thresholding function within 3D ROI manager was used to eliminate background signal.

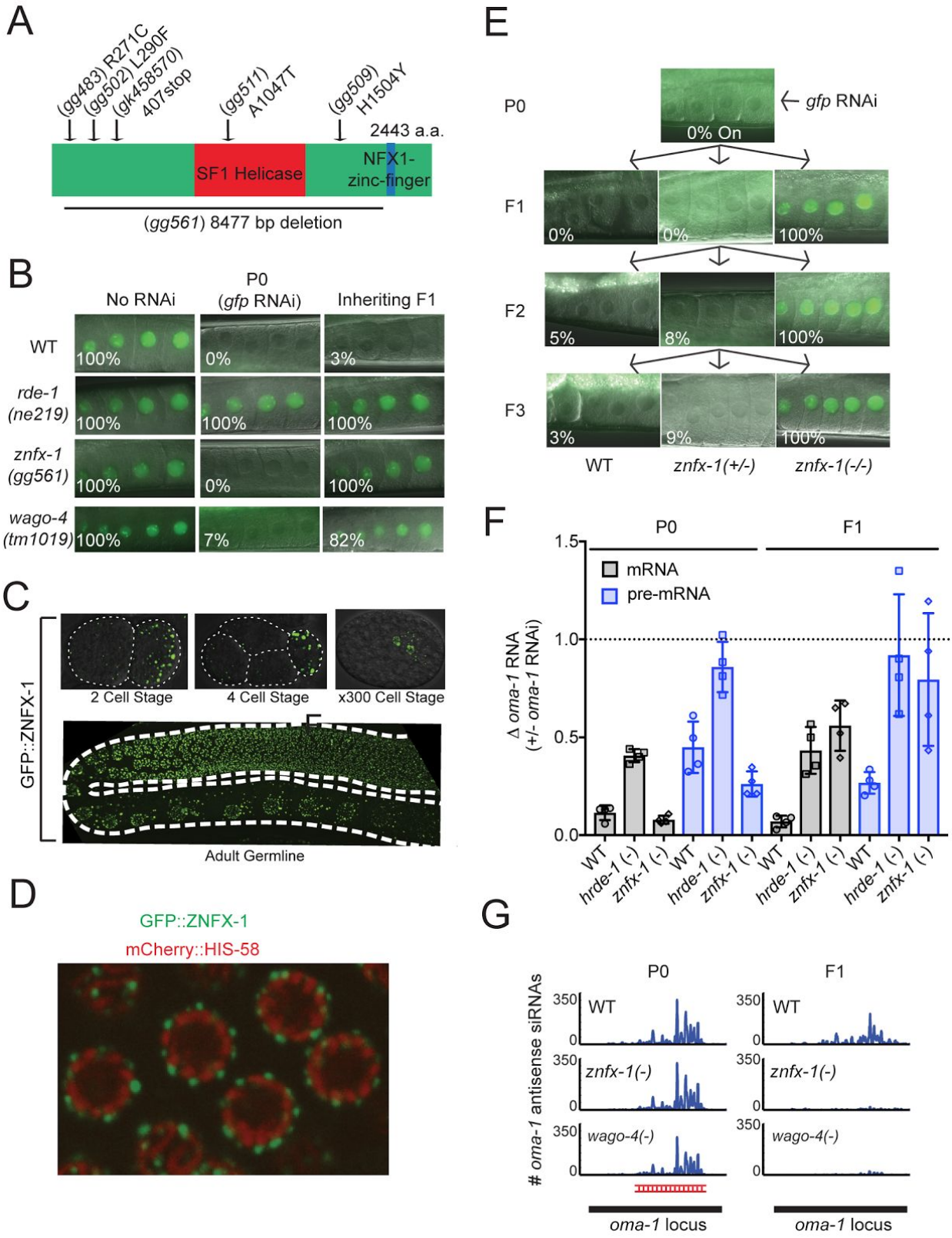

Figure 1. ZNFX-1 is a conserved RNA helicase required for RNAi inheritance in *C. elegans*. A) *znfx-1* alleles are indicated. **B)** Animals expressing a *pie-1::gfp::h2b* transgene[7]

were exposed to *gfp* dsRNA. F1 progeny were grown in the absence of dsRNA, and GFP expression in oocytes was visualized by fluorescence microscopy. % of animals expressing *pie-1::gfp::h2b* is shown. P0, parental generation; WT, wild-type. **C)** Animals harboring a *gfp* epitope inserted into the *znfx-1* locus were visualized by fluorescence microscopy. **D)** Pachytene germ cells of animals expressing GFP::ZNFX-1 and the chromatin marker mCherry::HIS-58 [24] were visualized by fluorescence microscopy. **E)** *znfx-1*(*gg561)*/+ heterozygous animals expressing *pie-1::gfp::h2b* transgene were exposed to *gfp* dsRNA. Progeny were grown in absence of *gfp* dsRNA for three generations. Images show GFP expression in oocytes. % of animals expressing *pie-1::gfp::h2b* is shown. **F)** WT, *hrde-1(tm1200)*, and *znfx-1(gg561)* animals were exposed to *oma-1* dsRNA. Total RNA from RNAi (P0) and inheriting (F1) generations was isolated. *oma-1* mRNA levels were quantified using qRT-PCR. n=4. Error bars are +/- standard deviation of the mean (SD). **G)** Secondary siRNA libraries (material and methods) were prepared from WT, *znfx-1(gg561)*, and *wago-4(tm1019)* animals exposed to *oma-1* dsRNA (P0) and progeny of these animals (F1). Antisense reads mapping to *oma-1* locus are shown. Red indicates region of *oma-1* targeted by dsRNA. Reads counts were normalized to total number of sequenced reads.

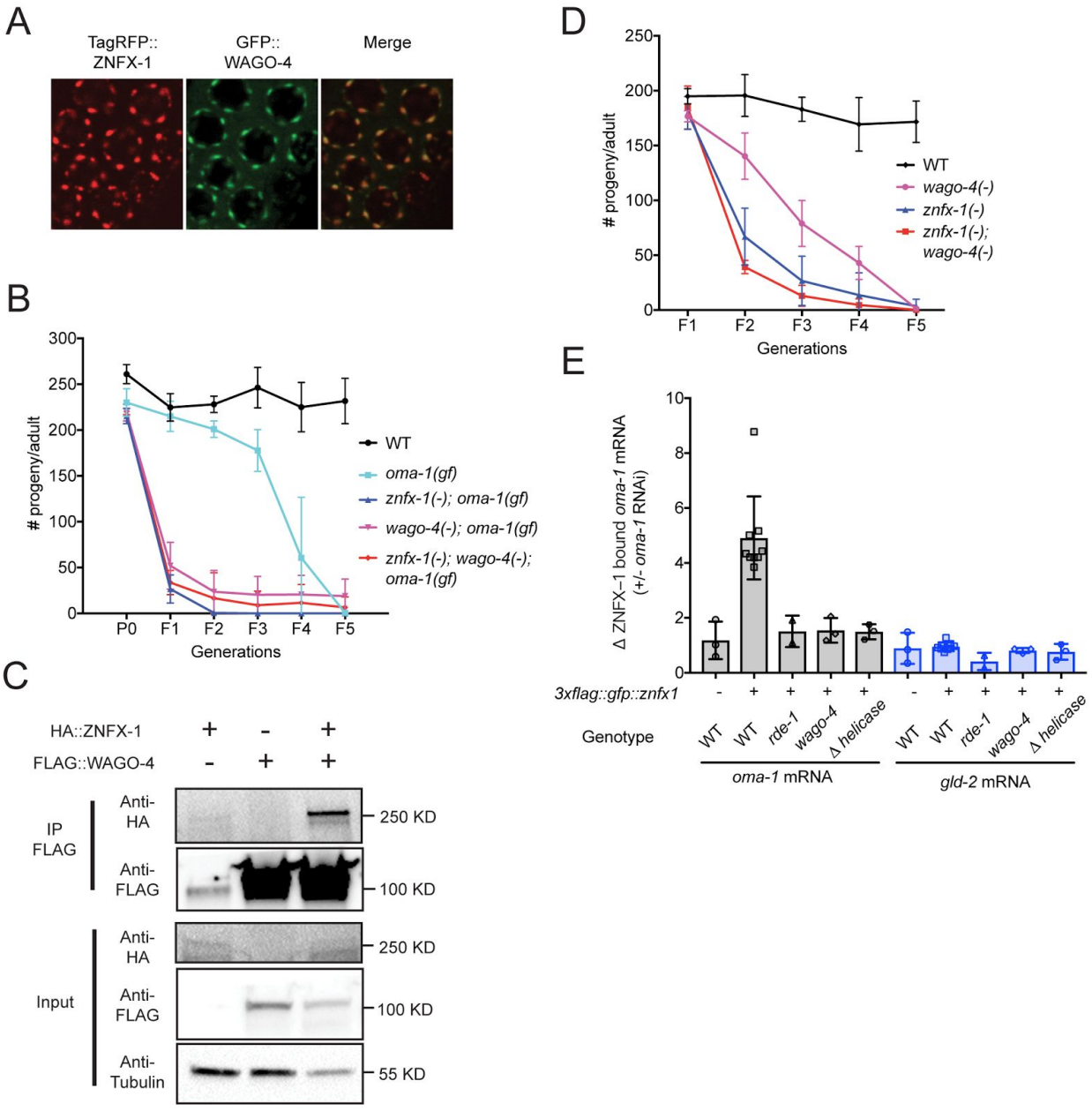

Figure 2. ZNFX-1 and WAGO-4 act cooperatively to drive RNAi inheritance. A) Fluorescent micrographs of pachytene germ cells of animals expressing GFP::WAGO-4 and TagRFP::ZNFX-1. **B)** *oma-1(zu405)* (*gf*) is a gain of function temperature sensitive allele of *oma-1*. *oma-1(gf)* animals die at 20C unless *oma-1(gf)* is silenced by *oma-1* RNAi, which is heritable [4]. *znfx-1(gg561)*, *wago-4(tm1019)*, and double mutant animals are similarly defective for *oma-1(gf)* RNAi inheritance (n=3. +/- SD). **C)** CoIP analysis of animals expressing *ha* or *3xflag* tags appended to *znfx-1* or *wago-4* loci, respectively (n=2). KD (Kilodaltons). **D)** Wild-type, *znfx-1(gg561)*, and *wago-4(tm1019), znfx-1(gg561); wago-4(tm1019)* animals were shifted to growth at 25°C in the P0 generation (not shown). Progeny were counted for five generations (F1-F5) (n=3. +/- SD). **E)** Wild-type or 3xFLAG::ZNFX-1 expressing animals were

treated with *oma-1* dsRNA. ZNFX-1 was IP'ed with α-FLAG antibodies and co-precipitating RNA was subjected to qRT-PCR to quantify *oma-1* mRNA co-precipitating with ZNFX-1 in wild-type, *rde-1(ne219)*, or *wago-4(tm1019)* animals. Δ *helicase* indicates 3xFLAG::ZNFX-1 containing a 1487 bp deletion, which removes (in frame) the helicase domain of ZNFX-1, was assayed for *oma-1* mRNA binding. *gld-2* is a germline expressed control mRNA. n=2 for *rde-1*, n=3-9 for others. +/- SD.

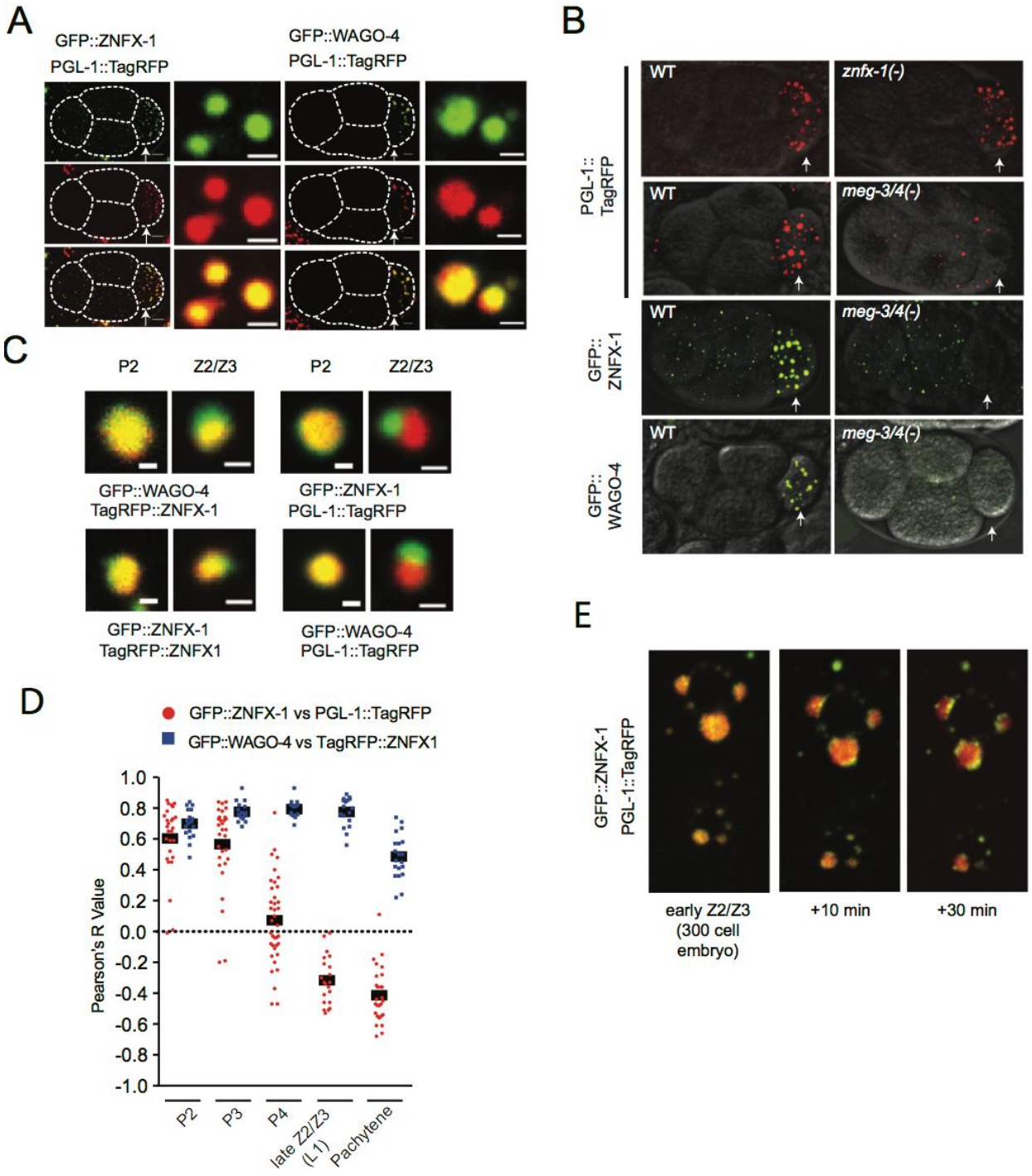

Figure 3. ZNFX-1 and WAGO-4 demix from P granule components during early embryogenesis. A-B) Micrographs of 4 cells embryos expressing indicated proteins are shown. P2 blastomeres are indicated by arrowheads. **A)** Magnifications of P granules are shown to the right. **B)** wild-type (WT), *znfx-1(gg561)*, or *meg-3(tm4259); meg-4(ax2026)*. **C)**

Magnifications of a P granule from a P2 blastomere and ZNFX-1/PGL-1 foci from Z2/Z3 cells from a larval stage one animal expressing indicated fluorescent proteins. **D)** Co-localization between GFP::WAGO-4 and TagRFP::ZNFX-1 (blue points) or GFP::ZNFX-1 and PGL-1::TagRFP (red points) was measured in individual granules at the indicated stages of development (see methods). Each data point represents an individual granule measurement (n = 15-35). **E)** Time-lapse micrographs of PGL-1::TagRFP and GFP::ZNFX-1 in early (~300 cell embryos) Z2/Z3 cells. Scale bars: **(A)** whole embryo 6 μm, individual granules 1 μm, **(C)** 0.5 μm.

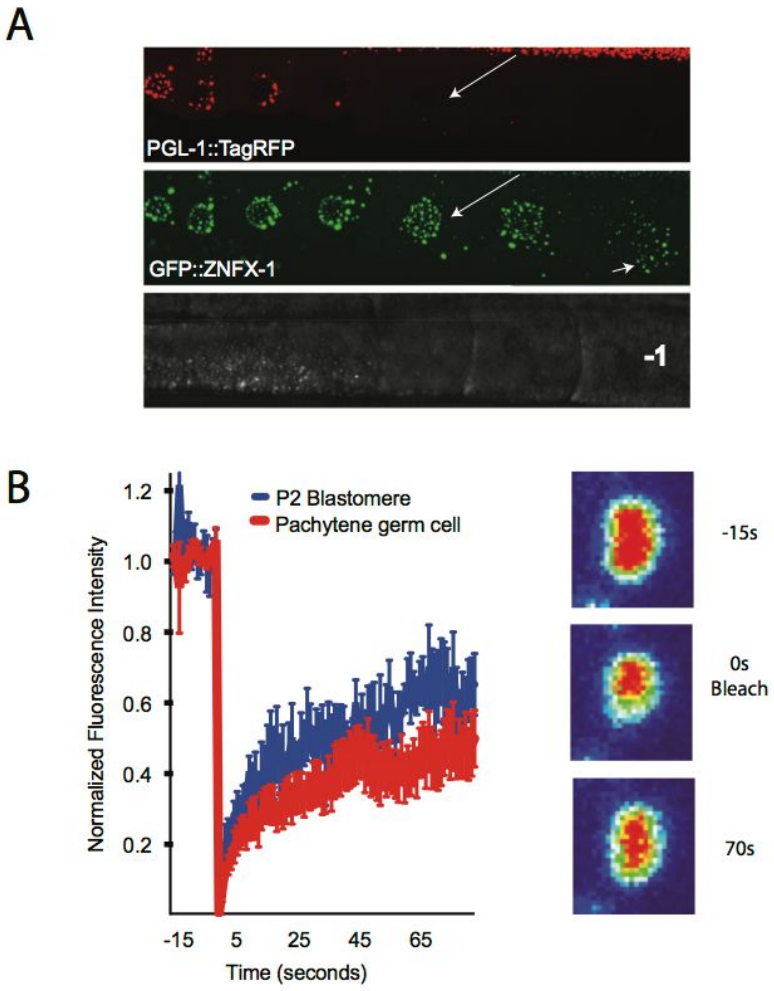

Figure 4. ZNFX-1/WAGO-4 foci are liquid droplet organelles. A) Maturing oocytes of animals expressing the indicated fluorescent proteins. Long arrows indicates oocyte that contains Z granule but not P granule. Short arrow indicates Z granules flowing off the nucleus and throughout the cytoplasm. -1 indicates -1 oocyte. **B)** GFP::ZNFX-1 expressing animals were subjected to FRAP (see methods) and GFP fluorescence was monitored in bleached area over indicated times. Data is normalized to a non-bleached control granule from same sample. n = 7 granules +/- SEM. Right, heat maps (red represents high GFP signal) showing recovery of ZNFX-1 fluorescence in a representative bleached Z granule.

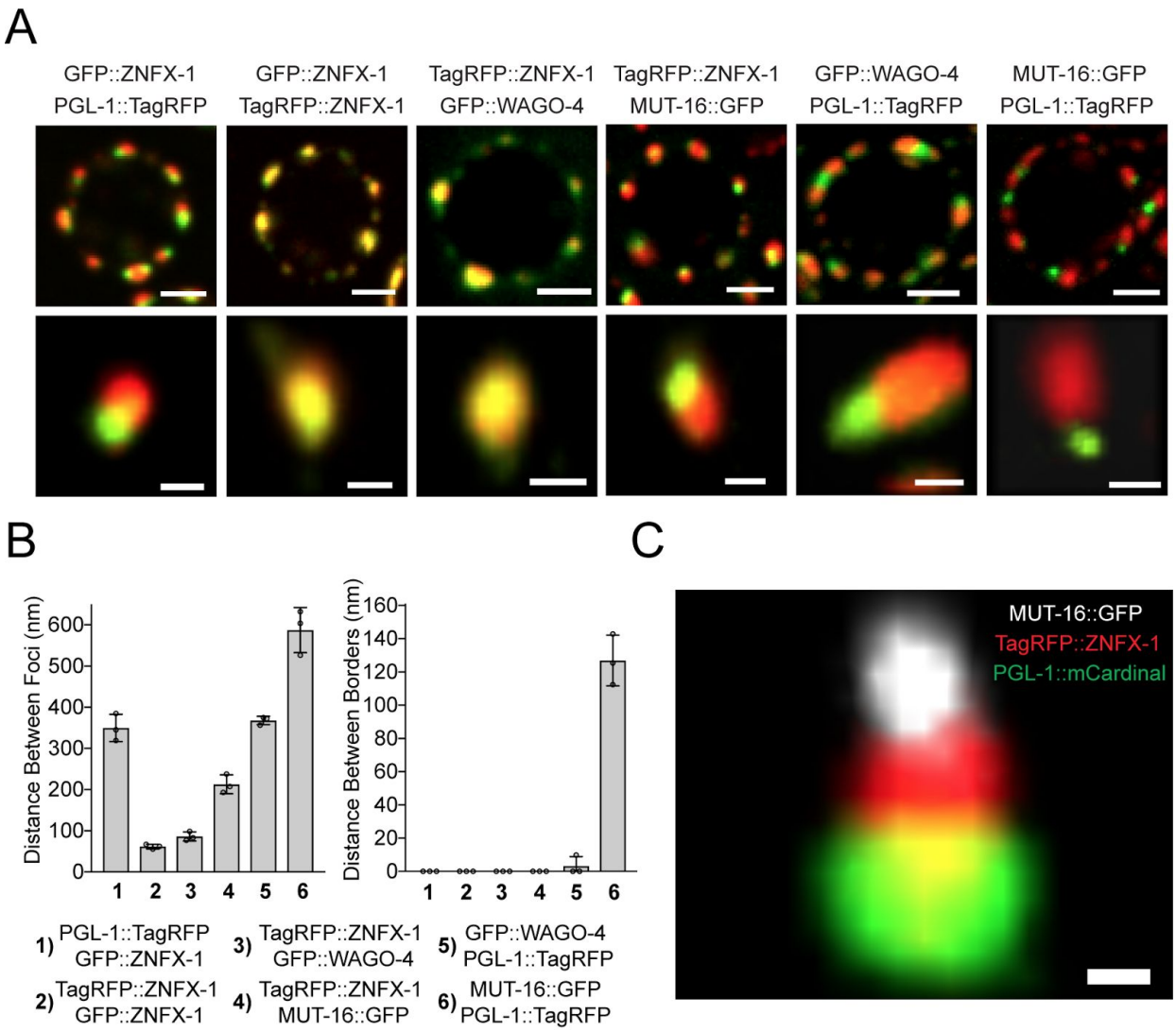

Figure 5. Z granules assemble into tri-droplet PZM structures with P granules and *Mutator* foci. A) Fluorescent micrographs of a single pachytene germ cell nucleus from animals expressing the indicated fluorescent proteins. 3D renders of representative foci are shown below. **B)** Distance between the centers (left) and surfaces (right) of the spaces occupied by the indicated fluorescent proteins was calculated as described in Methods. n= 3 (10 granules per sample) +/- SD. **C)** Fluorescent micrograph from pachytene region germ cell. Image is magnification of a single tri-droplet assembly (PZM). Green=PGL-1::mCardinal, Red=TagRFP::ZNFX-1, and white=MUT-16 ::GFP. Scale bars: **(A)** germ cell, 2 µm, single granule, 0.5 µm. **(C)** 0.25 µm. Position of nuclear membrane/nuclear pores with respect to each PZM segment is not known.